

# Predicting ozone depletion using $\text{BIn}_2\text{O}_3$ with RH based solid conductometric sensor

Sivasankari B.<sup>1</sup>, Ahilan A.<sup>2</sup>, Rajakumar S.<sup>3</sup> and Raja Kumar R.<sup>4</sup>

<sup>1</sup>Department of Electronics and Communication Engineering, SNS College of Technology, Saravanampatti, Coimbatore - 641035, Tamil Nadu, India

<sup>2</sup>Department of Electronics and Communication Engineering, PSN College of Engineering and Technology, Tirunelveli - 628851, Tamil Nadu, India

<sup>3</sup>Department of Electronics & Communication Engineering, Panimalar Engineering College, Chennai - 600123, Tamil Nadu, India

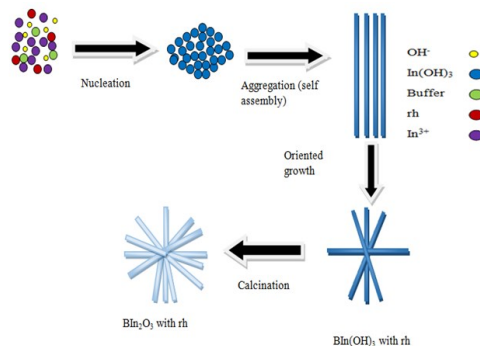
<sup>4</sup>Department of Maths, Sathyabama Institute of Science and Technology, Chennai - 600119, Tamil Nadu, India

Received: 20/10/2023, Accepted: 14/01/2024, Available online: 08/02/2024

\*to whom all correspondence should be addressed: e-mail: sivasankari235@outlook.com

<https://doi.org/10.30955/gnj.005457>

## Graphical abstract



## Abstract

Ozone depletion arises due to the presence of gases like chlorofluorocarbons and halons which are liberated into the atmosphere. The region of earth's atmosphere named as ozone shield, in which absorbs the ultra violet radiations of the sun. Although, its thickness varies periodically, this layer is primarily located in the lower stratosphere between 15 to 35 kms above the earth. Due to this, the ultraviolet rays directly enter into the earth causes harmful effects little by little on both living and non-living organisms. In this paper,  $\text{BIn}_2\text{O}_3$  with rh sensor in co precipitation method is used to detect the ozone depletion and it is based on the solid-state gas sensors. To achieve the excellent performance of an ozone depletion detecting branch like  $\text{BIn}_2\text{O}_3$  with rh, this was designed using a simple precipitation method. The coprecipitation method had deposited in  $\text{BIn}_2\text{O}_3$  with a thickness of 45 to 50 nanometer. The detection limit of ozone reduced as 30 parts per billion. Further, the gas detector demonstrated high sensitivity and selectivity of the device. The rhodium covers the surface areas ranges from 0 to 0.1. It reaches the accuracy of 96%. According to the degree of rhodium coverage, the sensors will be response to the ozone gas. The oxygen chemisorbed ability and a coverage of a great surface area of  $\text{BIn}_2\text{O}_3$  with rhodium highly related to the excellent sensing behavior. This study paves the way for an exact sensing and ppb level detection ozone gas.

**Keywords:** ozone depletion, gas sensor,  $\text{BIn}_2\text{O}_3$ , rhodium, CO precipitation.

## 1. Introduction

Ozone ( $\text{O}_3$ ) layer plays a vital role for surviving life on earth, because it acts like a barrier to oppose the ultra violet radiation which is present in the concentration level from 8ppm (parts per million) at a related height of 30km (kilometer) (Jayachandiran *et al.* 2020; Sui *et al.* 2021). The ozone gas is present in the stratosphere means it is good for the earth, because it's trying to block the ultraviolet rays until the ozone gas is in the lower atmosphere like troposphere means its causes some health affects like asthma and lung diseases to human beings (Onofre *et al.* 2019; Sun *et al.* 2019). The Figure 1 depicts the process of ozone depletion.

In accordance with (world health organization) WHO recommends that regulates the maximum concentration and timing of human exposure to ozone gas is limited to 50 ppb (parts per billion) to every 7 hours (Agathokleous *et al.* 2023; Adler and Severnini 2023). In this case ozone gas monitoring is very essential for preventing the people from human risks (Neale *et al.* 2023). The environmental quality of air is categorized into four levels as follows in terms of ozone such as excellent level means the ppb ranges from 0-50; good level means 50-100 ppb; poor level means 100-200 ppb and very poor means greater than 210 ppb (Mahmoud *et al.* 2023; Hertig *et al.* 2023). The level of noise in the background naturally is 30ppb (Zheng *et al.* 2023). Thus, it is quite important to tracking the level of ozone gas in the air because, it poses a concern to public health and the environment, since they can harm the respiratory system, causing a loss in lung function, inflammation of the airways, and discomfort (Breitner-Busch *et al.* 2023; Boshoman *et al.* 2023). In the gaseous form the ozone ( $\text{O}_3$ ) gas with the greater parts per billion and parts per million ranges is likely to detect or sense with the solid state conducto-metric sensors based on semiconductor oxide films like  $\text{In}_2\text{O}_3$ ,  $\text{WO}_3$  and rhodium (Amorello *et al.* 2023). These oxides are based on negative

type semiconductor and the ozone gas concentration is inversely related to its conductance in the atmosphere (Taylor *et al.* 2021). The rhodium is combined with the metal oxides, because it is a platinum group metals and mainly used for increasing the stability of the device. It's also used to change the characteristics of the metal oxides (Zhou *et al.* 2021). In this study branch like  $\text{In}_2\text{O}_3$  ( $\text{BIn}_2\text{O}_3$ ) with rhodium like nano materials are designed by using the co precipitation method (Sivasankari *et al.* 2022; Sheeja and Nishant, 2023). In this paper,  $\text{BIn}_2\text{O}_3$  with rh sensor in co precipitation method is used to detect the ozone depletion and it is based on the solid-state gas sensors. The major contribution of the work has been followed by,

- To achieve the excellent performance of an ozone depletion detecting branch like  $\text{BIn}_2\text{O}_3$  with rh, this was designed using a simple precipitation method.
- The coprecipitation method had deposited in  $\text{BIn}_2\text{O}_3$  with a thickness of 45 to 50 nanometer.
- The detection limit of ozone reduced as 30 parts per billion. Further, the gas detector demonstrated high sensitivity and selectivity of the device.

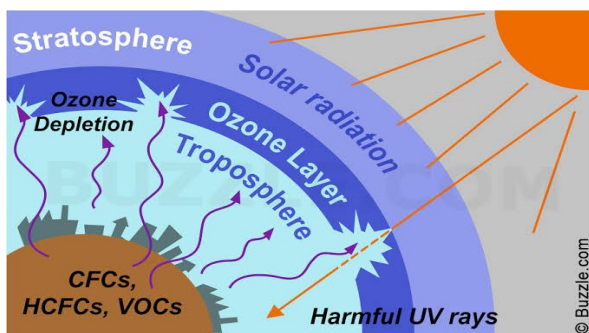


Figure 1. Ozone depletion process

## 2. Related works

In Avansi Jr *et al.* (2019) had proposed metal oxide nanostructures with a one-dimensional (1D) framework that can be applied in gas sensor devices. Here, hetero structures are involved to combine the variety of semiconducting nano materials with different energy bands effectively to enhance the effectiveness of the gas sensing system (Shiny *et al.* 2021). It looks into the chemical resistive sensing properties of a mixture of titanium dioxide ( $\text{TiO}_2$ ) nano materials and vanadium oxide ( $\text{V}_2\text{O}_5$ ) nanowires made by hydrothermal treatment of protometal complexes. A detection range of this sensor is (0.09-1.25 ppm) and it has good sensing features such as stability and selectivity but, little complex for designing the sensors.

In Staerz *et al.* (2018) had proposed an ozone gas sensor based on rhodium mixed with tungsten oxide and stannic oxide by investigating the material with some tests are xray diffract and direct current resistance. The addition of oxygen is adding to the rhodium clusters based on the standard sensing conditions. It identifies similarities across various supporting resources, as well as sample-specific characteristics also considered but missing the properties of base materials.

In levlev *et al.* (2018) had developed a palladium oxide material is involved to design the ozone gas sensors. For ozone gas and nitrogen oxide gas detection palladium oxide films are ready to oxygenation at a temperature range of 870 to 900 kelvin had demonstrated the good sensitivity, stability, operating speed. During the tests of sensitivities to various nitrogen dioxides and ozone concentrations at low temperatures, this combined structure reaches the maximum sensitivity and operating speed. The palladium oxide sensors can detect ozone gas and can be employed in the field of public medical care and the habitat. Because the synthesis approach is relatively simple and compatible with planar technologies used in the microelectronic industry, palladium oxide nanostructures have a strong possibility of becoming one of the key materials for commercial manufacture of oxidizing gas sensors.

In Joshi *et al.* (2019) had developed the detection of ozone gas by using the ultra violet supported chemical resistive sensors with gold plate of zinc oxide nanorods and it is based on hypothermal method. Under ultra violet radiation, the chemical resistive sensor is normally working at 1volt at room temperature. In comparison to certain other oxidization and reduction gases, the sensing characteristics are stable, repeatable, and selective for ozone gas. The gold with zinc oxide nanorods with dimensions ranging from 68 to 350 nanometers and height of the rod ranging from 1 to 3 meters. Here in missing to calculate the variations of gold thickness corresponding to its effects on the performance of the sensor.

In Buelvas *et al.* (2023) provides an analysis of the data quality associated with Internet of Things-based air quality monitoring devices. The main characteristics of Data Quality (DQ) and the corresponding methods for improving DQ have been identified via the use of a systematic mapping technique and by consulting existing standards for assessing data quality in these systems. After analyzing more than 70 publications, we found that the use of different calibration procedures improves accuracy and precision, two DQ elements that are commonly addressed by diverse works. Based on our research, we present a discussion of the problems that must be overcome to improve data quality in Internet of Things (IoT)-based air quality monitoring systems.

In Smiy *et al.* (2020) suggested utilizing the drop coating approach to create gas sensors based on thin films perovskite type substrate with interdigitated Ptelectrodes. The sol-gel process was used to generate the perovskite starting nanoparticles, which have an orthorhombic structure and pnma space group. The created thin film responds promisingly when evaluated as a sensitive film for ozone detection. The produced thin film is a possible ozone detection sensor since it detects low concentrations of ozone.

In Petani *et al.* (2020) developments in the field of ozone sensor technology. Ozone gas sensors and dissolved ozone sensors are two categories of sensors. Thus, the emphasis is on optical, amperometric, and impedimetric measuring techniques. It presents the advancements made in a

number of categories, including reaction time, recovery time, measuring temperature, and measurement range. An overview of the existing methods for inkjet-printed ozone

sensors is included in this study, as inkjet printing is a novel and promising technology for embedding sensors in medical and bioanalytical equipment.

Author and Year	Proposed	strengths	weaknesses
In 2019 Avansi Jr W.,	proposed metal oxide nanostructures with a one-dimensional (1D) framework that can be applied in gas sensor devices	Heterostructures can be designed to exhibit enhanced sensitivity to ozone.	This limitation could impact the ability to tailor the sensor for optimal performance.
In 2018 Staerz A.,	proposed a ozone gas sensor based on rhodium	SMOX-based sensors to be effectively used in the future, their sensitivity, selectivity, and stability must be increased	Rhodium is a precious metal, and its oxide is relatively expensive.
In 2018 Ievlev V.M.,	developed a palladium oxide material	advantageous for applications like catalysis and sensing, where increased surface area enhances reactivity or sensitivity.	Palladium is a precious metal, and its cost can be relatively high.
In 2019 Joshi N.,	developed the detection of ozone gas	UV-assisted chemiresistors can enable selective sensing by promoting specific reactions or interactions between target molecules and the sensing materials under UV illumination.	Implementing UV-assisted chemiresistors often involves a more complex design and fabrication process.
In 2023 Buelvas, J.,	analysis of the data quality associated with Internet of Things-based air quality monitoring devices	good sensitivity of our sensor especially at the operating temperature of 170 degree	However, for a concentration above 120 ppb in the atmosphere, Ozone could cause serious health problems
In 2020 Smiy S.	utilizing the drop coating approach to create gas sensors based on thin films perovskite type substrate with interdigitated Ptelectrodes	improve data quality in IoT-based air quality monitoring systems	Internet of Things (IoT), there has been an increase in the deployment of low-cost air quality monitoring systems
In 2020 Petani L.,	developments in ozone sensor technology	is increasing interest in the utilisation of medical gases, such as ozone, for the treatment of herniated disks, peripheral artery diseases, and chronic wounds, and for dentistry	potential side effects and in some cases they do not even relieve the pain

2.1. Differences between proposed and current approaches

The key findings of their study, as well as the differences between the existing and suggested techniques, are summarized below.

1. Another factor that renders present approaches inappropriate for certain real-time applications is computational complexity. The proposed model, on the other hand, was shown to be computationally efficient.

3. Proposed method

3.1. Chemical materials

The various materials involved such as 99 percent of indium hydroxide, 1 ml of rhodium, 89 percent of buffer can be used for block the ph value changes. Here, cetyl trimethyl ammonium bromide is used as a buffer. For combining all these materials by using co precipitation method. To form the  $\text{BiIn}_2\text{O}_3$  with rhodium several processes take under like nucleation, aggregation and calcination.

3.2. Synthesis process

When a new material phase begins to form, the nucleation process takes precedence. This might be a crystal structure that emerges as a substance begins to solidify, or it could be what happens when a gas transitions from a gaseous to a liquid state, and in this case, the heterogeneous nucleation process is appropriate to enable the other components. In 60milliliter of deionized water is dissolved in 86 milligram of indium nitrate. The combinations of hydroxides, rhodium, indium and cetyl trimethyl ammonium bromide buffer is combining to form molecules of indium hydroxides. Schematic diagram for the formation of  $\text{BiIn}_2\text{O}_3$  with rhodium shown in Figure 2.

The ultraphonic was used for 30 minutes after adding 150 mg of cetyl trimethyl ammonium bromide to the solution. Drop by drop, 20milligram of freshly prepared and to the mixed solution, 0.1 milligram sodium borohydride dilute solution was added. The whitish samples were cleaned and

retrieved with methanol along with deionized aqueous solution later mixing the solution for 1 hour. Next, the indium hydroxides are subjected to the aggregation process in which crushed or collapsed the whole component and convert the one form into another. This stage, the materials forms rod like structure arranged in a parallel form into the corresponding weight. For improving the weights or length done by the oriented growth process. At last, the light yellowish precipitated element is dried through the night at 60degree Celsius. The precipitated element was annealed in an air environment at 598°Celsius for 2.5 hours at a temperature range of 1°C The calcinations is attributes to the presence of oxygen or air for heating to remove the unwanted particles.

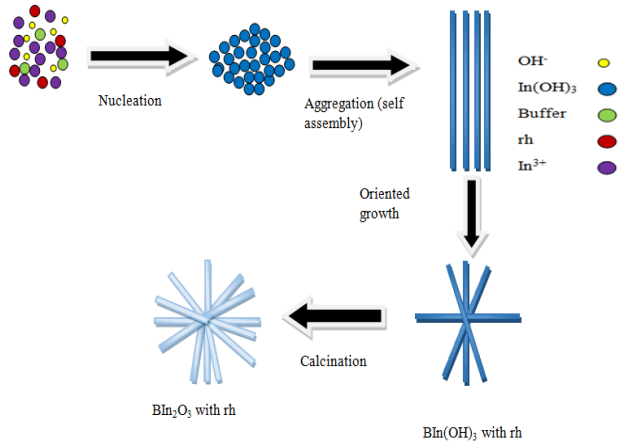


**Figure 2.** Block diagram for the formation of Bln<sub>2</sub>O<sub>3</sub> with rhodium

### 3.3. Characterization

The linking of sensors into the Bln<sub>2</sub>O<sub>3</sub> with rhodium is discussed below. The Bln<sub>2</sub>O<sub>3</sub> films were deposited at the temperatures of 340 to 380° celsius and 460 to 480° Celsius. These films are assigned as ht (high temperature) and lt (low temperature) films accordingly. The thickness of the Bln<sub>2</sub>O<sub>3</sub> was 35 to 60nanometer. The number of sensors for detecting oxidising gases, such as ozone, should be created with thicknesses. The gas diffusion's impact on sensor performance might be avoided. A formation of the crystallite having the average size in the low and high temperature films are 7 to 11nanometer and 12 to 18nanometer. A source of mini electron beam evaporation was used to deposit rhodium on the surface of the films. The degree of rhodium coverage was calculated and going to consideration the lack of continual rhodium layer on the Bln<sub>2</sub>O<sub>3</sub> surface.

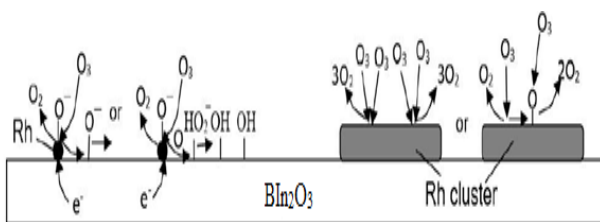


**Figure 3.** Pictorial depiction of the process takes place on Bln<sub>2</sub>O<sub>3</sub> with rhodium during ozone detection

The deposition time was used to adjust the thickness of the deposited rhodium. An oscillating glass microbalance instrument was used to determine the rate of deposition.

This indicates that after 50 seconds of evaporation, a coating comparable to 0.1 ml of rhodium was formed.

The above Figure 3 depicts the processes takes place on the Bln<sub>2</sub>O<sub>3</sub> with rh based sensor during ozone gas detection. A flow through the measuring cell is used to test the Bln<sub>2</sub>O<sub>3</sub> with rh based sensor. The cell volume was 0.3 cm, allowing for gas-sensitive effects to be controlled with time constants larger than 3–5sec. The concentration of the test gas was 1 part per million. The relative humidity in air was maintain at the range of 40 to 50 percent. The sensors' operating temperatures varied between 30-to-450-degree celsius and noting that the structural characteristics of Bln<sub>2</sub>O<sub>3</sub> films remained consistent throughout these tests. The maximal sensitivity of ozone was discovered at temperatures of 200 to 250° Celsius as a consequence of studying gas sensing qualities. The main measurement was carried at a temperature of 250° celsius. The resistance and sensitivity readings of the sensors were promptly gathered by the analysis method. The responsivity of the sensor is expressed as equation (1). The responsivity of the sensor is relating to the ratio of the sensor's resistance in the atmosphere with ozone gas to the resistance of the sensor in atmosphere without ozone gas.

$$r = \frac{r_{ozone}}{r_{air}} \quad (1)$$

The time constant was calculated using the stable state value of layer conductance at the 0.9 level of transient processes such as responsivity and recovery time. The metrics were taken after the sensors were artificially aged, which comprised a series of tests using reduction and oxidation gases at a temperature of 400° celsius.

### 3.4. Coprecipitation model

Coprecipitation is a method used to precipitate one or more substances from a mixture by the addition of a precipitating reagent. This process involves the formation of a new compound between the precipitating reagent and the substance(s) being precipitated. Coprecipitation can be used in various applications, including the separation and purification of chemicals, the removal of pollutants, and the recovery of valuable materials. The method is typically carried out at high temperatures and/or with strong acids or bases. The coprecipitation method is a technique commonly used in chemistry for the synthesis of nanoparticles or the separation of specific ions from solution. While it has several advantages, it also comes with certain limitations. Here are some of the limitations of the coprecipitation methods such as Particle Size and Agglomeration, Poor Reproducibility, Purity Issues, Limited Control Over Crystal Structure etc.

## 4. Result and discussion

When examining the rhodium modified films and note that their semisolid conductometric response to ozone follows the same general rules as intrinsic films. Here analyse effect of rhodium surface alteration on the actual values of the sensitivity to ozone, as well as the time that it takes for this reaction to happen. Figure 4 shows the impact of alteration of the rhodium surface on the response of a Bln<sub>2</sub>O<sub>3</sub> based

semi-solid conductivity gas sensor at a temperature of 250° celsius. The suggested technique is implemented using MATLAB2020b running on a Windows 10 OS with an Intel i3 core processor at 2.10 GHz and 8GB RAM. No, the proposed model of these conditions is not representative of real-world scenarios

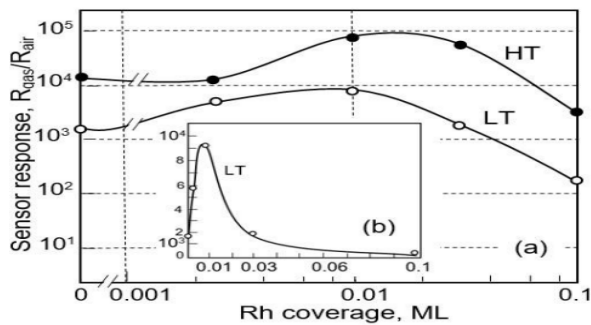


**Figure 4.** Impact of alteration of the surfaces of high and low temperature  $\text{BiIn}_2\text{O}_3$  with rhodium on their conductometric response to ozone

The Figure 5 depicts the impact of alteration of the surfaces on the conductivity of  $\text{BiIn}_2\text{O}_3$  layers calculated in an air in presence or along with absence of ozone ( $\text{O}_3$ ) gas.

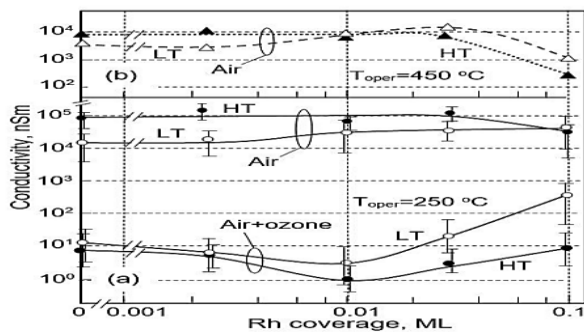


**Figure 5.** Change in the conductivity of high and low temperature of  $\text{BiIn}_2\text{O}_3$  with rhodium layers later alterations of the surfaces with rhodium, calculated in an air and ozone ( $\text{O}_3$ ) at a temperature (a) 250degree celcius (b) 450degree celcius

Here, behaviour of the sensor response of rhodium modified  $\text{BiIn}_2\text{O}_3$  films related to its characteristics of the rhodium. The responsivity of the sensing device with rhodium altered  $\text{BiIn}_2\text{O}_3$  has a rhodium covered area on the layer has a well-defined limit of 0.01 ml. The covered area and the sensing device responses are inversely proportional to each other.

The rhodium is behaving as an enhancer of the interface of ozone's with the surfaces of  $\text{BiIn}_2\text{O}_3$  at low levels of surface coverage and the greater the degree of coverage, the more it acts as a catalytically active filter, preventing ozone interactions with  $\text{BiIn}_2\text{O}_3$ . The impact of rhodium surfaces alteration on the gas sensor qualities of  $\text{BiIn}_2\text{O}_3$  films is dependent on the film's fundamental properties. Especially, the  $\text{BiIn}_2\text{O}_3$  with rhodium films formed at high temperature and have more sensitive to ozone. More importantly, the nature of the impact of rhodium surface alteration on sensor properties is independent of the  $\text{BiIn}_2\text{O}_3$  film deposition temperature, which boosts the credibility of the results obtained. The rhodium coverage is larger than 0.01 to 0.02 ml, means the sensor response drops. As previously stated, an increase in the size of

rhodium nano particles causes a decrease in binding energy. If the rhodium on the surface of  $\text{BiIn}_2\text{O}_3$  is in the atomic state, or near to it, with coverage of less than 0.01 ml, the development of 3dimension clusters occurs in the rhodium covered area surpasses 0.01 ml. The size of these 3dimension clusters grows when the rhodium coating on the  $\text{BiIn}_2\text{O}_3$  surface is increased, reaching 1 to 2 nanometers with 0.1 ml of rhodium.  $\text{Rh}_2\text{O}_3$  films are formed when rhodium is deposited in an ozone environment at the temperature of 200°celcius. This indicates the  $\text{Rh}^{3+}$  phase is the almost possible rhodium phase in a rhodium bunch in an oxygen ( $\text{O}_2$ ) rich environment at the temperature of less than 300°celcius. If a probable variation in the charge charge phase of rhodium (Rh) interface with ozone ( $\text{O}_3$ ), if it occurs  $\text{Rh}^{3+} \leftrightarrow \text{Rh}^{4+}$  while switching from one oxide phase to another phase  $\text{RhO}_2 \leftrightarrow \text{Rh}_2\text{O}_3$ , then the response of the sensor should not be affected. It is known that  $\text{Rh}_2\text{O}_3$  and  $\text{RhO}_2$  are steady in an oxygen rich environment. This indicates that the  $\text{RhO}_2 \leftrightarrow \text{Rh}_2\text{O}_3$  transition and it is irreversible under the influence of ozone. As a result, if do not utilise the reducing gas in this research, this  $\text{RhO}_2 \leftrightarrow \text{Rh}_2\text{O}_3$  transition should arise only once after the initial encounter of the  $\text{BiIn}_2\text{O}_3$  with rhodium film with ozone, and it should not appear again during future contacts with ozone. When looks at the influence of  $\text{BiIn}_2\text{O}_3$  alteration of the surfaces with rhodium layers their conductance valuated in different atmospheres and find that changes in film conductivity later the alterations of the surfaces with rhodium are negligible, when calculated in air without ozone ( $\text{O}_3$ ). Based on the obtained behaviour patterns and deduce that ozone adsorption on rhodium in a simple state or close to the simple state is accompaniment by exchange of electrons between the oxides of metal and chemisorbant oxygen, which is caused by dissociative ozone adsorption started by atom of rhodium. The synthesis of ozonide ion radicals can be used to described this process  $\text{O}_3^-$  and its consequent degradation into monoatomic and diatomic oxygen species in eqn (2)



The variation in conductance of  $\text{BiIn}_2\text{O}_3$  with rhodium layers based on the action of rhodium, determined in an ozone environment, was thus observed. The rise in the density of ionised oxygen species on the metal oxide's surface causes the metal oxide's resistance to increase when it interacts with ozone. The results of the investigation of the kinetics of the responsivity of the sensor are shown in Figure 6. While the response and recovery periods for low temperature films are essentially unaffected by the rhodium surface modification, the influence of rhodium on the kinetics of the sensor response is seen at the response time and recovery time for high temperature  $\text{BiIn}_2\text{O}_3$  films at 225° celsius.

An attempt was made to analyze the cross sensitivity of  $\text{BiIn}_2\text{O}_3$  to oxygen, ozone and water. Furthermore, the settings under which these studies were carried out are very various from the actual operating parameters of gas sensors. The primary alterations in high temperature films



occur in the range of 0.01 ml of rhodium. This supports our theory that there is a shift in the mechanism of the process that causes the sensor response when rhodium is present.

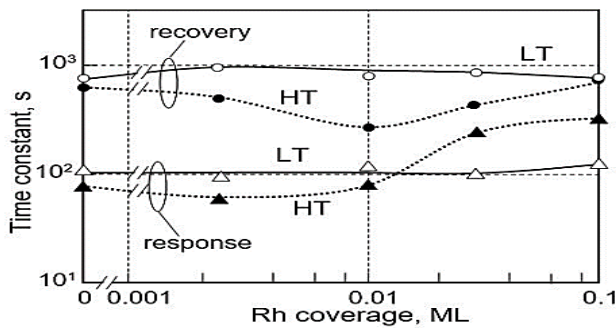


**Figure 6.** Effect of surface modification of low and high temperature  $\text{Bi}_2\text{O}_3$  film with rhodium on the time constants of the sensor response to the ozone

The electrical response of the  $\text{Bi}_2\text{O}_3$  with rhodium sample was studied at a constant operating temp for 1 minute while exposed to 560 ppb of ozone gas. The best sensor response was achieved at 200 C, which is similar to that of typical gas sensors are depicted in the Figure 7.

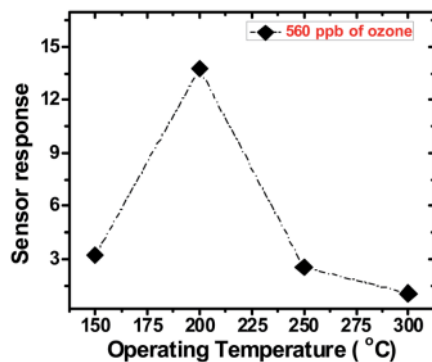


**Figure 7.** Gas sensing response of  $\text{Bi}_2\text{O}_3$  exposed to 560 ppb  $\text{O}_3$  at different operating temperatures

The Figure 8 (a, b) shows the response of the sensor for  $\text{Bi}_2\text{O}_3$  platelets as a function of ozone concentrations. One of the most significant factors for hazardous gas sensor applications is response and recovery time.

As the concentration rises from 28 to 165 ppb, the reaction time enhances from 32 to 48 seconds and the recovery time from 1 to 6.5 minutes. In comparison to greater concentrations, more ozone molecules easily interact with adsorbed oxygen ions at low concentrations, resulting in a faster reaction.

**Table 1.** Compares the parameters of ozone gas with other metal oxides

sensors	method	Detection of ozone limit(ppb)	working temperatures (degree celcius)	recovery times	response times
ZnO	Hydrothermal method	60-1000	250	15 sec	60 sec
$\text{WO}_3$	RF-sputtering	30-800	260	17 sec	1200 sec
$\text{SnO}_2$	Spray pyrolysis deposition	1000	280	20 sec	150 sec
$\text{NiCo}_2\text{O}_4$	Polymeric precursor	30-900	300	24 sec	200 sec
$\text{Bi}_2\text{O}_3$	Co-precipitation	28-165	200	25 sec	62 sec

## 5. Conclusion

As a consequence,  $\text{Bi}_2\text{O}_3$  with rhodium nanoparticles were effectively produced using the coprecipitation approach, which was clear and simple to use. When compared to

These resistance changes are substantially less than those seen with ozone, indicating that ozone may be detected selectively using  $\text{Bi}_2\text{O}_3$  platelets.

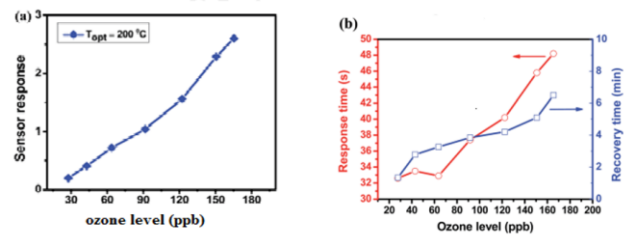


**Figure 8.** (a) Sensor response vs gas concentration. (b) Gas sensing response and recovery time

The Table 1 reliefs the comparing the parameters for ozone sensing  $\text{Bi}_2\text{O}_3$  with rhodium in other traditional ozone gas sensors, including  $\text{WO}_3$ ,  $\text{ZnO}$ ,  $\text{SnO}_2$ ,  $\text{NiCo}_2\text{O}_4$ . From the knowledge, the sensor described here was capable of detecting the lowest level of ozone for the temperature while maintaining optimal performance.

The proposed methodology is run in a highly scalable platform to tackle large-scale challenges. The dimensions of the several test functions range from 30 to 50, 50 to 80, and 80 to 100. In Figure 9, the performance of the suggested model exhibits a variety of behaviors, demonstrating the resilience of the proposed approach. It has also been discovered that when used in a highly scalable setting, the performance decrease is minimal.

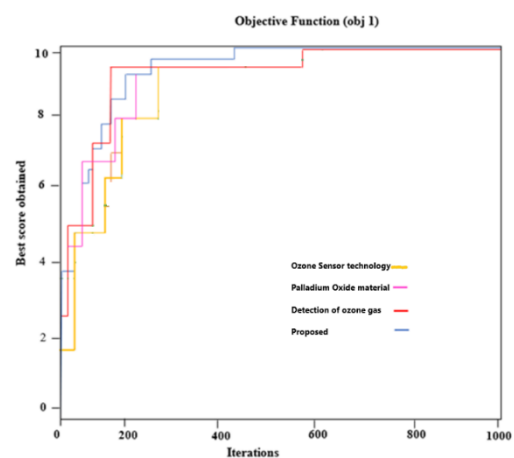


**Figure 9.** Scalability analysis

commercial-powder-based sensors, the results of ozone sensing using  $\text{Bi}_2\text{O}_3$  with rhodium nanomaterials were dramatically improved, with greater responsiveness and faster response and recovery speeds. The impact produced when rhodium is employed to change the surface of films

$\text{Bi}_2\text{O}_3$  developed for use in gas sensors aiming at ozone detection has a significant size-dependent character. If any rise in the responsivity of the sensor to ozone ( $\text{O}_3$ ) can be achieved at low covered areas, then alterations of the  $\text{Bi}_2\text{O}_3$  surface with rhodium at large covered areas will project a result responsivity of the sensor. It reaches the accuracy of 96%. This impact is linked to the shift of rhodium from an atomically scattered phase to a 3dimension bunch phase on the surface of  $\text{Bi}_2\text{O}_3$ , as well as a varying in the mechanics of interface of rhodium with ozone ( $\text{O}_3$ ) and  $\text{Bi}_2\text{O}_3$ . Future research will focus on developing the network architecture and data processing protocols required to support the evolving paradigm of air pollution monitoring by fostering trust in the low-cost technology's dependability.

## References

- Adler D. and Severnini E. (2023). Timing matters: Intra-day shifts of economic activity and ambient ozone concentrations, *Journal of Public Economics*, **223**, 104905.
- Agathokleous S., Saitanis C.J., Savvides C., Sicard P., Agathokleous E. and De Marco, A. (2023). Spatiotemporal variations of ozone exposure and its risks to vegetation and human health in Cyprus: an analysis across a gradient of altitudes, *Journal of Forestry Research*, **34**(3), 579–594.
- Amorello D., Orecchio S., Barreca S. and Orecchio S. (2023). Voltammetry for Monitoring Platinum, Palladium and Rhodium in Environmental and Food Matrices. *ChemistrySelect*, **8**(18), e202300200.
- Avansi Jr W., Catto A.C., da Silva L.F., Fiorido T., Bernardini S., Mastelaro V.R., Aguir K. and Arenal R. (2019). One-dimensional  $\text{V}_2\text{O}_5/\text{TiO}_2$  heterostructures for chemiresistive ozone sensors, *ACS Applied Nano Materials*, **2**(8), 4756–4764.
- Boshoman S.B., Fatoba O.S. and Jen T.C. (2023). Transition metal oxides as electrocatalytic material in fuel cells: a review, *Engineered Science*, **25**, 948.
- Breitner-Busch S., Mücke H.G., Schneider A. and Hertig E. (2023). Impact of climate change on non-communicable diseases due to increased ambient air pollution, *Journal of Health Monitoring*, **8**(Suppl 4), 103.
- Buelvas J., Múnera D., Tobón V, D.P., Aguirre J. and Gaviria N. (2023). Data quality in IoT-based air quality monitoring systems: a systematic mapping study. *Water, Air, & Soil Pollution*, **234**(4), 248.
- Hertig E., Hunger I., Kaspar-Ott I., Matzarakis A., Niemann H., Schulte-Droesch L. and Voss M. (2023). Climate change and public health in Germany—An introduction to the German status report on climate change and health 2023, *Journal of Health Monitoring*, **8**(Suppl 3), 6.
- Ievlev V.M., Ryabtsev S.V., Samoylov A.M., Shaposhnik A.V., Kushev S.B. and Sinelnikov A.A. (2018). Thin and ultrathin films of palladium oxide for oxidizing gases detection, *Sensors and Actuators B: Chemical*, **255**, 1335–1342.
- Jayachandiran J., Arivanandhan M., Padmaraj O., Jayavel R. and Nedumaran D. (2020). Investigation on ozone-sensing characteristics of surface sensitive hybrid rGO/WO<sub>3</sub> nanocomposite films at ambient temperature, *Advanced Composites and Hybrid Materials*, **3**(1), 16–30.
- Joshi N., da Silva L.F., Shimizu F.M., Mastelaro V.R., M'Peko J.C., Lin L. and Oliveira O.N. (2019). UV-assisted chemiresistors made with gold-modified ZnO nanorods to detect ozone gas at room temperature. *Microchimica Acta*, **186**(7), 1–9.
- Mahmoud M.A., Abo Laban G.F., Ibrahim I.S., El-Dessouki W.A., Metwaly K.H., Saba R.M. and Zahra, A.A. (2023). Influence of ozone gas on the khapra beetle, *Trogoderma granarium* (Coleoptera: Dermestidae) in stored wheat, *Applied Entomology and Zoology*, **58**(2), 181–191.
- Neale P.J., Williamson C.E., Banaszak A.T., Häder D.P., Hylander S., Ossola R., Rose K.C., Wängberg S.Å. and Zepp R. (2023). The response of aquatic ecosystems to the interactive effects of stratospheric ozone depletion, UV radiation, and climate change, *Photochemical & Photobiological Sciences*, 1–35.
- Onofre Y.J., Catto A.C., Bernardini S., Fiorido T., Aguir K., Longo E., Mastelaro V.R., da Silva L.F. and de Godoy M.P. (2019). Highly selective ozone gas sensor based on nanocrystalline ZnO.  $\text{ZnO}$  thin film obtained via spray pyrolysis technique, *Applied Surface Science*, **478**, 347–354.
- Petani L., Koker L., Herrmann J., Hagenmeyer V., Gengenbach U. and Pylatiuk C. (2020). Recent developments in ozone sensor technology for medical applications, *Micromachines*, **11**(6), 624.
- Sheeja R. and Nishant R. (2023). Reduction in greenhouse gas emission by using sustainable transportation systems to increase the environmental and economic benefits, *International Journal of System Design and Computing*, **01**(01), 18–25.
- Shiny, G. S., Ragaventhiran, J., Islabudeen, M., Sharmila, G. and Kumar, B. M. (2021). WITHDRAWN: Heterogeneous wireless sensor networks (HWSN) and its energy efficient protocols A correlative study.
- Sivasankari B., Ahilan A., Jeyam A., and JasmineáGnamamalar A. (2022). Care living instrument for neonatal infant connectivity solution (CLiNicS) in smart environment, *Journal of Ambient Intelligence and Smart Environments*, (Preprint), 1–14.
- Smiy S., Bejar M., Dhahri E., Fiorido T., Bendahan M. and Aguir K. (2020). Ozone detection based on nanostructured  $\text{La}_0.8\text{Pb}_0.1\text{Ca}_0.1\text{Fe}_0.8\text{Co}_0.2\text{O}_3$  thin films, *Journal of Alloys and Compounds*, **829**, 154596.
- Staerz A., Boehme I., Degler D., Bahri M., Doronkin D.E., Zimina A., Brinkmann H., Herrmann S., Junker B., Ersen, O. and Grunwaldt J.D. (2018). Rhodium oxide surface-loaded gas sensors, *Nanomaterials*, **8**(11), 892.
- Sui N., Zhang P., Zhou T. and Zhang T. (2021). Selective ppb-level ozone gas sensor based on hierarchical branch-like  $\text{In}_2\text{O}_3$  nanostructure, *Sensors and Actuators B: Chemical*, **336**, 129612.
- Sun Q., Wu Z., Cao Y., Guo J., Long M., Duan H. and Jia D. (2019). Chemiresistive sensor arrays based on noncovalently functionalized multi-walled carbon nanotubes for ozone detection, *Sensors and Actuators B: Chemical*, **297**, 126689.
- Taylor G., Shallenberger J., Tint S., Fones A., Hamilton H., Yu L., Amini S. and Hettinger J. (2021). Investigation of iridium, ruthenium, rhodium, and palladium binary metal oxide solid solution thin films for implantable neural interfacing applications, *Surface and Coatings Technology*, **426**, 127803.
- Zheng D., Huang J., Fang Y., Deng Y., Peng C. and Dehaen W. (2023). Fluorescent Probes for Ozone-Specific Recognition: An Historical Overview and Future Perspectives, *Trends in Environmental Analytical Chemistry*, e00201.
- Zhou K.L., Wang Z., Han C.B. Ke X., Wang C., Jin Y., Zhang Q., Liu J., Wang H. and Yan H. (2021). Platinum single-atom catalyst coupled with transition metal/metal oxide heterostructure for accelerating alkaline hydrogen evolution reaction, *Nature Communications*, **12**(1), 3783.